Chapter 17

Different Levels of Exhumation across the Bucaramanga Fault in the Cepitá Area of the Southwestern Santander Massif, Colombia: Implications for the Tectonic Evolution of the Northern Andes in Northwestern South America

Sergio AMAYA–FERREIRA[1]* , Carlos Augusto ZULUAGA[2] , and Matthias BERNET[3]

1 samaya@sgc.gov.co, samayaf@unal.edu.co
Servicio Geológico Colombiano
Dirección de Recursos Minerales
Diagonal 53 n.° 34–53
Bogotá, Colombia

2 cazuluagacas@unal.edu.co
Universidad Nacional de Colombia
Sede Bogotá
Departamento de Geociencias
Carrera 30 n.° 45–03
Bogotá, Colombia

3 matthias.bernet@univ-grenoble-alpes.fr
Université Grenoble Alpes
Insitut des Sciences de la Terre
1381 rue de la piscine, CS 40700, 38058
Grenoble cedex 9, France

* Corresponding author

Abstract Apatite and zircon fission–track data from crystalline rocks collected along an east–to–west elevational profile across the Bucaramanga strike–slip fault in the Cepitá area and thermal history modeling show the four–stage thermal history of the southwestern Santander Massif of the northern Andes in Colombia. A 60 my phase of burial heating from the Late Jurassic to the Late Cretaceous was followed by three cooling phases beginning in approximately 65–60 Ma, which were related to regional tectonic events. The Late Cretaceous – early Paleocene accretion of an island arc and interactions of the Caribbean Plate with the northwestern South America plate first triggered the surface uplift and erosional exhumation of the Santander Massif. During the late Oligocene – early Miocene, the collision of the Panamá–Chocó Block with northwestern South America caused an acceleration in the cooling and exhumation of the Santander Massif and differential surface uplift to the east and west of the Bucaramanga Fault in the Cepitá area. The present–day topography of the Santander Massif probably formed at that time. Locally recorded late Miocene cooling may be related to movement on the secondary fault pattern in the study area or minor magmatic activity.

Keywords: exhumation, fission–track analysis, Santander Massif, Bucaramanga Fault, thermal modeling.

Resumen Datos de huellas de fisión en apatito y zircón de rocas cristalinas colectadas a lo largo de un perfil de elevación este–oeste a través de la Falla de Bucaramanga, falla de rumbo, en el área de Cepitá y el modelamiento de la historia termal muestran una historia termal en cuatro etapas para el suroeste del Macizo de Santander de los Andes del norte en Colombia. A los 60 millones de años, una fase de calentamiento por enterramiento desde el Jurásico Tardío al Cretácico Tardío fue seguida por tres fases de enfriamiento que comenzaron aproximadamente a los 65–60 Ma, y están relacionadas con eventos tectónicos regionales. En el Cretácico Tardío–Paleoceno temprano, la acreción de un arco de islas y las interacciones de la Placa del Caribe con el noroccidente de la Placa de Suramérica desencadenaron el primer levantamiento de superficie y la

Quaternary

Neogene

Paleogene

Cretaceous

Jurassic

Triassic

Permian

Carboniferous

Devonian

Silurian

Ordovician

Cambrian

Proterozoic

exhumación erosiva del Macizo de Santander. Durante el final del Oligoceno y el Mioceno temprano, la colisión del Bloque Panamá–Chocó con el noroeste de Suramérica provocó la aceleración del enfriamiento y de la exhumación del Macizo de Santander y la elevación diferencial de la superficie al este y al oeste de la Falla de Bucaramanga en el área de Cepitá. Probablemente, la topografía actual del Macizo de Santander se formó en ese momento. El enfriamiento del Mioceno tardío registrado localmente puede estar relacionado con el movimiento en el patrón de falla secundaria en el área de estudio o con la actividad magmática menor.

Palabras clave: *exhumación, análisis de huellas de fisión, Macizo de Santander, Falla de Bucaramanga, modelamiento termal.*

1. Introduction

The rise of orogenic mountain belts, particularly in the northern Andes, has a significant influence on regional climate and atmospheric circulation and precipitation patterns, and forms barriers to species migration and the creation of new habitats and ecological niches (e.g., Hoorn et al., 2010; Mapes et al., 2003). For paleogeographic reconstructions, it is important to link the exhumation of deep–seated crystalline rocks and the formation of high orogenic topography with the plate–tectonic evolution of the area of interest. Here, we present a study on the exhumation history of the southern Santander Massif in northeastern Colombia because this mountain belt holds a key position in the northern Andes, forming the northwest–striking continuation of the Eastern Cordillera at the junction between the Eastern Cordillera and the Mérida Andes in Venezuela to the east (Figure 1). The Santander Massif is part of the so–called Maracaibo Block, which is delineated by the Santa Marta–Bucaramanga and Oca strike–slip Fault Systems and the southwestern fold–and–thrust belt of the Mérida Andes (Figure 1; e.g., Colletta et al., 1997; Mann et al., 2006). The Maracaibo Block also includes the Sierra Nevada de Santa Marta and the serranía de Perijá (Figure 1). The cooling history of the crystalline rocks of the central and southern Santander Massif has been previously studied with low–temperature thermochronology, with apatite fission–track (AFT) ages ranging from 20 to 7 Ma and zircon fission–track (ZFT) ages ranging from 172 to 20 Ma (Amaya et al., 2017; Shagam et al., 1984; van der Lelij et al., 2016; Villagómez et al., 2011). In addition, from outcrops to the east of the city of Bucaramanga and the Bucaramanga Fault, Mora et al. (2015) first presented AHe ages between 8.2 and 16 Ma and ZHe ages between 22.6 and 24.2 Ma. Along the same profile, Amaya et al. (2017) demonstrated an exhumed ZFT partial annealing zone, which was rapidly exhumed between 25 and 20 Ma. All these data show the importance of late Oligocene regional tectonics driving the exhumation of the Santander Massif along the Bucaramanga Fault, which is related to the break–up of the Farallón Plate and the collision of the Panamá–Chocó Block with northwestern South America (Farris et al., 2011; Taboada et al., 2000; O'Dea et al., 2016). This regional tectonic influence has already been shown in the exhumation of the Antioquian

Batholith in the Central Cordillera (Restrepo–Moreno et al., 2009). Parra et al. (2012) argued, on the basis of AFT data from the Nuevo Mundo Syncline sedimentary basin fill and thermal modeling, for a Paleocene – early Eocene (60–50 Ma) phase of pronounced shortening and cooling of the western margin of the Eastern Cordillera associated with tectonic inversion and the first surface uplift and erosion of the Eastern Cordillera. However, the Parra et al. (2012) study lacked information from ZFT or zircon (U–Th)/He thermochronometers and therefore the pre–depositional thermal histories in their models were fully unconstrained. Regardless, the absence of Cretaceous sedimentary cover rocks in large areas of the Santander Massif, which are otherwise widespread in the Eastern Cordillera of Colombia, suggests erosion was an important process during the exhumation history of the Santander Massif. Evidence of Paleogene and Neogene erosional exhumation of the Santander Massif basement and sedimentary cover rocks is preserved in the stratigraphic sequences of the Lisama, La Paz, Esmeraldas, Mugrosa, Colorado, and Real Formations in the Nuevo Mundo, Armas, and Andes Synclines of the Middle Magdalena Valley (Figure 1; Caballero et al., 2013; Parra et al., 2012; Sánchez et al., 2012). Deformation of the Middle Magdalena Valley area probably began during the Paleocene, with structures such as the Lisama Anticline (Caballero et al., 2013).

The objective of this study was to more precisely constrain the exhumation history of the southwestern Santander Massif in the Cepitá area, to the east and west of the Chicamocha River (Figure 2). Thus far, very few and spatially dispersed thermochronological data have been published from this region (Caballero et al., 2013; Shagam et al., 1984; van der Lelij et al., 2016). Therefore, we present data of 10 AFT and 9 ZFT samples collected from igneous and metamorphic crystalline rocks along a profile across the Chicamocha Canyon and the Bucaramanga Fault System near Cepitá, referred to here as the western and eastern blocks of the Santander Massif (Figures 2, 3), respectively. The Chicamocha River does not exactly follow the trace of the Bucaramanga Fault System but does mark the present–day morphologic separation between the two blocks. While the western block reaches an elevation of only approximately 1600 m in the study area, the eastern block rises to more than 3200 m in this part of the Santander Massif (Figure 3). Expo-
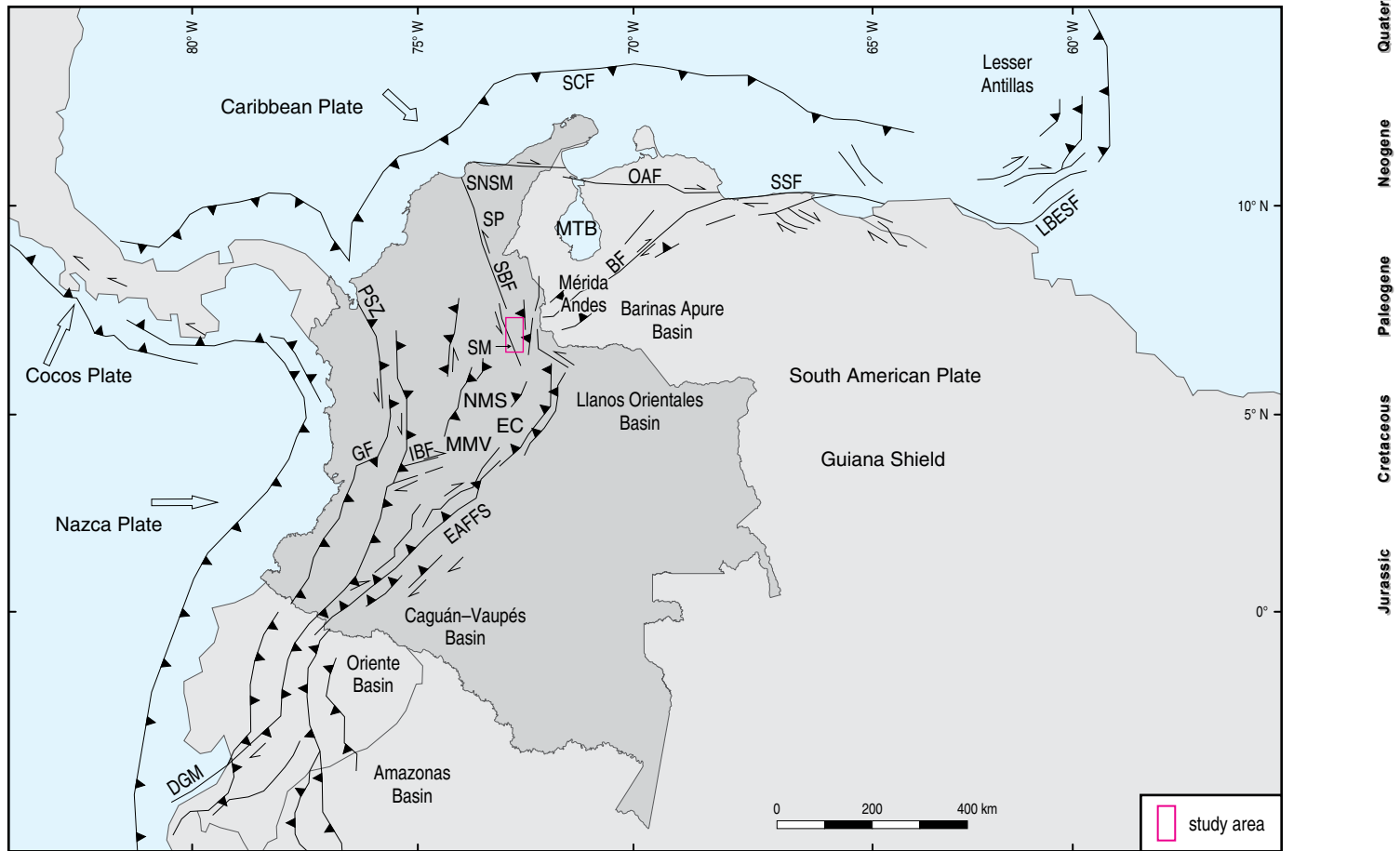
Figure 1. Overview map showing the major tectonic features of northern South America (modified from Colmenares & Zoback, 2003). (SCF) Southern Caribbean Marginal Fault; (SNSM) Sierra Nevada de Santa Marta; (OAF) Oca–Ancón Fault; (SSF) San Sebastián Fault System; (LBESF) Los Bajos–El Soldado Fault System; (SP) serranía de Perijá; (MTB) Maracaibo Triangular Block; (SBF) Santa Marta–Bucaramanga Fault; (BF) Boconó Fault; (PSZ) Panamá suture zone; (SM) Santander Massif; (GF) Garrapatas Fault; (IBF) Ibagué Fault; (NMS) Nuevo Mundo Syncline; (EC) Eastern Cordillera; (MMV) Middle Magdalena Valley; (EAFFS) Eastern Andean Front Fault System; (DGM) Dolores–Guayaquil Megashear.

sure of crystalline rocks at high surface elevations implies both exhumation and surface uplift. The thermochronological data of this study were used in t–T models to provide constraints on the timing of cooling. The cooling histories were then interpreted in terms of erosional and tectonic exhumation. To constrain the difference in relative surface uplift between the western and eastern blocks, ZFT cooling ages at similar elevations on both sides of the Bucaramanga Fault were compared. Furthermore, the apparent fission–track cooling ages were translated into exhumation rates (e.g., Willett & Brandon, 2013) for the crystalline rocks that were buried beneath sedimentary rocks at least since the Late Jurassic and throughout most of the Cretaceous.

2. Geological Setting

The fault–bounded triangular Maracaibo Block in the northern Andes is an interesting geological feature, as this block not only hosts the highest coastal mountain belt in the world including the 5700 m–high Pico Cristobal Colón of the Sierra Nevada de Santa Marta, but also features the Santander Massif, the serranía

de Perijá, and the Mérida Andes of Venezuela along two of its three sides (Figure 1). Even if two of the main bounding faults of the Maracaibo Block, the dextral Oca Fault to the north and the sinistral Santa Marta–Bucaramanga Fault on its western flank, are strike–slip fault systems with an unknown vertical offset, considerable topographic surface elevations have been attained in the Sierra Nevada de Santa Marta and the Santander Massif (up to 4530 m at Paramo del Almorzadero). The Santa Marta–Bucaramanga Fault extends for over 600 km from Santa Marta in the north to the Chicamocha Canyon, approximately 40–70 km south of Bucaramanga, where it ceases defining the western margin of the Santander Massif (Figure 1). The Boconó strike–slip fault dominates the late Miocene to Pliocene evolution and exhumation of the Mérida Andes of Venezuela (Bermúdez et al. 2010, 2011, 2013; Kohn et al. 1984), but the southeastern fold–and–thrust belt is thought to delimit the Maracaibo Block to the southeast against the South American continental plate (e.g., Figure 1; Colletta et al., 1997; Mann et al., 2006).

Late Proterozoic to Paleozoic metamorphic rocks intruded by Triassic and Jurassic plutonic rocks form the crystalline core
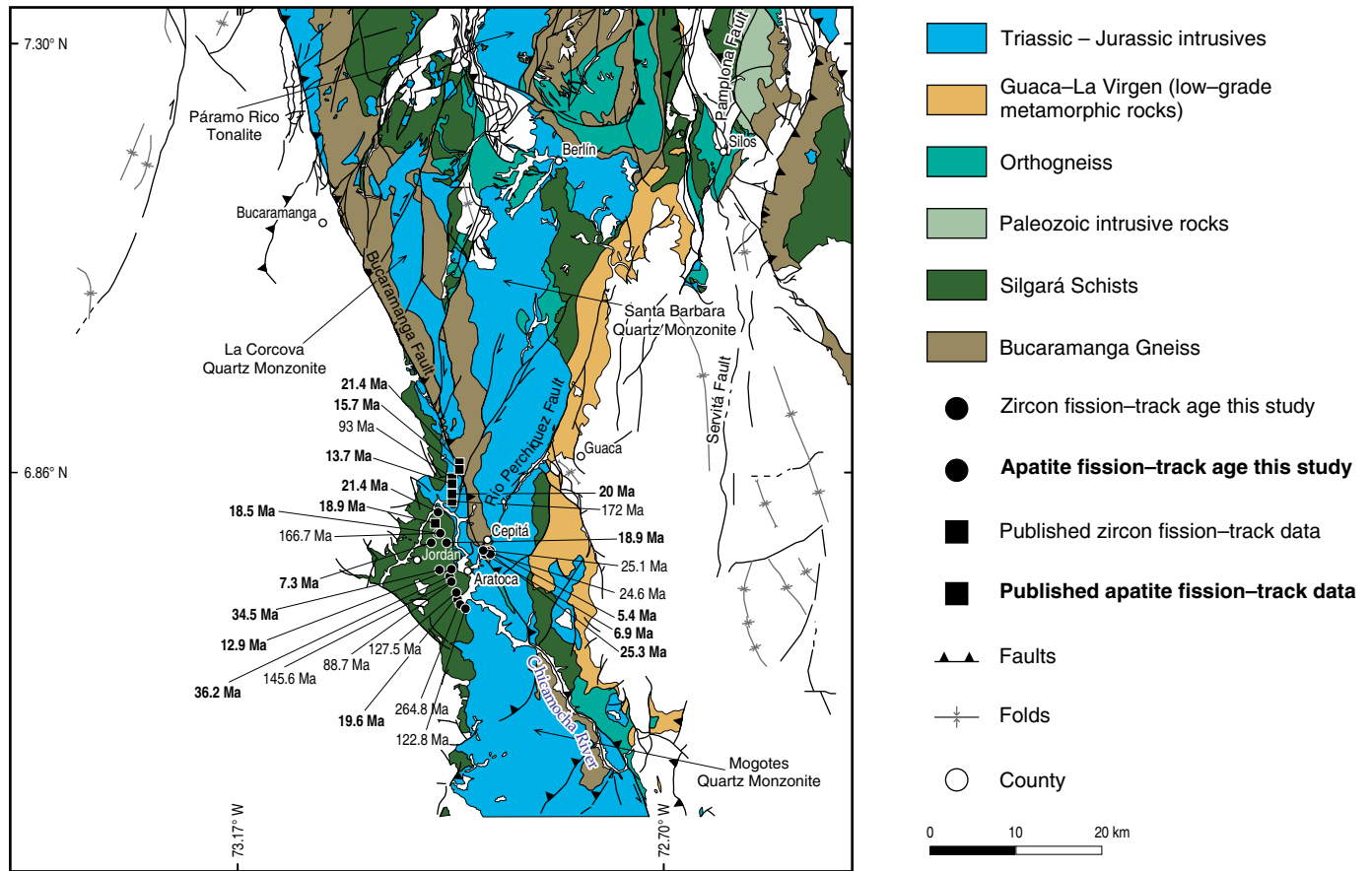
Figure 2. Geological map and sample locations. Taken and modified from Zuluaga & López (2018).
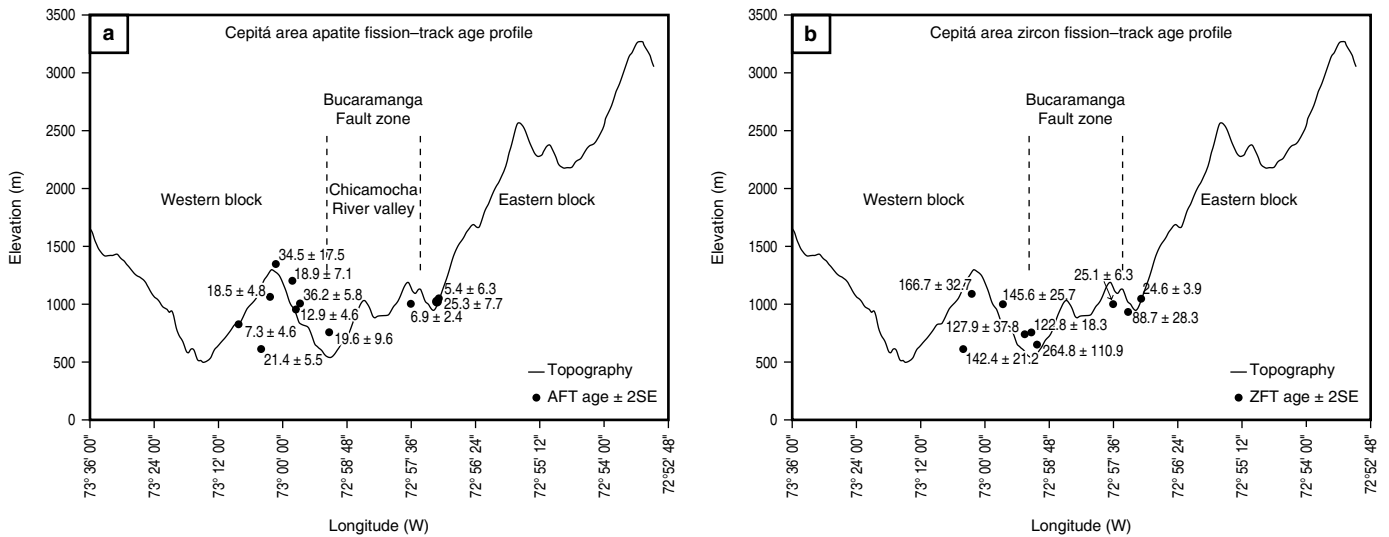

Figure 3. Topographic profile with sample locations.

of the Santander Massif (Goldsmith et al., 1971). In this study, only the late Proterozoic Bucaramanga Gneiss, Paleozoic Silgará Schists, Jurassic Mogotes Batholith and Pescadero Granite are of interest because samples were only collected from these lithological units to the east and west of the Chicamocha River

(Figures 2, 3). The Jurassic and Cretaceous sedimentary cover rocks, with a cumulative thickness of ca. 2500 to ca. 3500 m (Shagam et al., 1984), were used as a constraint for thermal history modeling for the phase and amplitude of the Jurassic and Cretaceous burial heating in the study area. A zircon fission

track age in the study area of 172.0 ± 16.4 Ma from the Pescadero Granite of van der Lelij et al. (2016) indicates that burial heating was insufficient to fully reset the zircon fission–track system to the west of the Bucaramanga Fault. Our samples of the western profile were collected between 612 and 1347 m elevation between Cepitá and Aratoca, whereas eastern profile samples were collected from elevations ranging between 900 and 1050 m to the east of Cepitá (Figure 2; Table 1).

The Chicamocha River is a tributary of the Magdalena River. In the Cepitá area, the Chicamocha River flows in a N–NW direction, before following the secondary NE–SW– oriented fault pattern of the Santander Massif and turning to the SW and flowing toward the village of Jordán (Figure 2). In the study area, the Chicamocha Canyon shows at least 1000 m of incision with respect to the highest elevations of the western block (Figure 3).

3. Methods

3.1. Fission–Track Analysis

Sample preparation for the fission–track analysis was completed at the Servicio Geológico Colombiano in Bogotá, following the methodology described by Amaya et al. (2017). All samples were irradiated at the FRM II research reactor in Garching, Germany. For track length measurements of horizontally confined tracks, apatite samples were irradiated with ^{252}Cf at the University of Melbourne. Samples were analyzed dry at 1250x with an Olympus BX51 optical microscope, using the FTStage 4.04 system of Trevor Dumitru in the fission–track laboratory of the Servicio Geológico Colombiano in Bogotá and in the fission–track laboratory at ISTerre, Université Grenoble Alpes.

3.2. Time–Temperature History Modeling

For t–T history modeling of the western profile samples, we used the QTQt program (v 4.6) of Gallagher (2012) to model age pairs of samples for which we have AFT and ZFT data and length measurements of horizontally confined tracks in apatite. The QTQt program determines cooling history scenarios using a Bayesian transdimensional Markov Chain Monte Carlo approach, which determines simple thermal history models to avoid over interpretation of the observed data (Gallagher, 2012). The output models were the maximum likelihood (best–fit) or expected (weighted mean from the posterior distribution) models. The program permits the insertion of constraint boxes to include other geological information on the timing of subsidence, burial, or exhumation in the model. AFT data are used to constrain a cooling history below 110 °C (Donelick et al., 2005). ZFT data can constrain the cooling history at temperatures below ca. 240 °C for radiation–damaged zircons and common orogenic cooling rates (e.g., Bernet, 2009; Brandon et al., 1998).

Our study also employed the most robust and revealing method plotting length against a kinetic parameter (Dpar), noting whether trends exist and, if possible, defining coherent kinetic populations (e.g., Burtner et al., 1994). This approach not only can result in more accurate age interpretation but also allows length data to be segregated to enable proper inverse modeling. Because fission–track lengths shorten as a function of the thermal history they have undergone, a set of length measurements constitutes an integrated record of the temperatures experienced by a sample.

3.3. Exhumation Rate Estimates

First–order exhumation rates based on AFT and ZFT ages can be estimated from the simple 1–D thermal advection model age2dot created by Mark BRANDON (see Ehlers et al., 2005). For these first–order estimates, we assumed a constant pre–exhumation thermal gradient of 30 °C/km, which we acknowledge is a very simplistic assumption but sufficient for the purpose of this study. The AFT model was selected for chlorine apatite, which is justifiable with regard to the measured Dpar values shown in Table 2. For the ZFT model, we selected annealing parameters for radiation–damaged zircon, given that the ZFT cooling ages are on average older than 100 Ma for the western block. For the eastern block samples 13SACZ03 and 07, we used a zero–damage model, considering that these zircons rapidly cooled below the zircon fission–track closure temperature and through the zircon partial annealing zone between 25 and 20 Ma (Table 3).

4. Results

4.1. Fission–Track Data

The samples from the western profile, to the west of the Chicamocha River and the Bucaramanga Fault zone, have AFT ages between 36 and 7 Ma depending on elevation (Figure 4a). The lowest sample, i.e., 12SACEP11 from the Silgará Schists, yields a central AFT age of 21.4 ± 5.5 Ma and was collected at 612 m along the secondary fault pattern of the Santander Massif (Figures 2, 3; Table 2). Sample 12SACEP16 from the Silgará Schists yields a central AFT age of 18.9 ± 7.1 Ma, with a mean Dpar value of 1.88 μm. Sample 12SACEP08 yields a central AFT age of 12.9 ± 4.6 Ma, with a mean Dpar value of 2.17 μm. The highest sample of the western block, i.e., 12SACEP17 from the Silgará Schists, was collected at 1347 m and has a central AFT age of 34.5 ± 17.5 Ma. The oldest AFT age in the western block, i.e., 36.2 ± 5.8 Ma, was recorded for sample 13SACZ01 at 945 m. Forty–nine horizontally confined track length measurements yielded an average c–axis projected track length of 13.84 ± 2.74 μm. The mean Dpar value of these samples is 1.92 μm.

Table 1. Fission–track samples, Cepitá area, Santander Massif.

Sample	Longitude (°W)	Latitude (°N)	Elevation (m)	Lithology	Stratigraphic unit
			Western block		
12SACEP02	–72.9838216	6.7535936	651	mica schist	Silgará Schists
12SACEP05	–72.9876257	6.7615073	741	amphibolite	Silgará Schists
12SACEP06	–72.9855766	6.7638081	757	mica schist	Silgará Schists
12SACEP08	–72.9954973	6.7778402	952	mica schist	Silgará Schists
12SACEP11	–73.0067275	6.8158368	612	mica schist	Silgará Schists
12SACEP13	–73.0137446	6.7962065	826	mica schist	Silgará Schists
12SACEP14	–73.0039793	6.8029836	1063	mica schist	Silgará Schists
12SACEP16	–72.9970256	6.7981493	1202	garnet–mica schist	Silgará Schists
12SACEP17	–73.0021697	6.7789128	1347	mica schist	Silgará Schists
13SACZ01	–72.9954700	6.7778000	954	amphibolite	Silgará Schists
13SACZ02	–72.9942340	6.7715950	1006	granite	Pescadero Granite
13SACZ09	–72.9831889	6.7597976	652	granite	Pescadero Granite
			Eastern block		
13SACZ03	–72.9514600	6.7744600	1050	quartz vein	Bucaramanga Gneiss
13SACZ04a	–72.9520300	6.7744000	1022	andesitic dike	Bucaramanga Gneiss
13SACZ04b	–72.9520300	6.7743618	1022	gneiss	Bucaramanga Gneiss
13SACZ05	–72.9555273	6.7735458	935	migmatite	Bucaramanga Gneiss
13SACZ07	–72.9601810	6.7795084	1003	gneiss	Bucaramanga Gneiss

Table 2. Santander Massif (Cepitá area) apatite fission–track data.

Sample	N	r_s (10^4 cm^{-2})	N_s	r_i (10^5 cm^{-2})	N_i	r_d (10^6 cm^{-2})	P(c²)	U (ppm)	Central Age (Ma)	±2σ	MDpar (μm)	±2σ	Length** (μm)	±2σ	n° length
						Western block									
12SACEP06	17	8.56	62	9.74	705	1.19	0.0	12	19.6	9.6	2.08	0.26	15.12	1.28	4
12SACEP08	20	5.53	38	7.08	486	1.19	19.4	9	12.9	4.6	2.17	0.19	15.11	1.19	11
12SACEP11	20	0.91	8	16.2	1420	1.19	0.9	20	21.4	5.5	1.94	0.18	15.64	0.76	55
12SACEP13	20	1.06	12	2.39	270	1.21	68.4	3	7.3	4.6	–	–	–	–	–
12SACEP14	20	6.13	74	5.46	659	1.20	55.9	7	18.5	4.8	–	–	–	–	–
12SACEP16	20	9.89	67	9.11	617	1.19	0.5	11	18.9	7.1	1.88	0.18	15.22	1.61	15
12SACEP17	20	3.07	20	1.46	95	1.20	80.5	2	34.5	17.5	1.98	0.26	14.00	1.51	11
13SACZ01*	20	4.26	49	1.96	225	1.10	80.4	3	36.2	5.8	1.92	0.20	13.84	2.74	49
						Eastern block									
13SACZ04a	20	10.7	80	27.3	2051	1.23	0.1	33	6.9	2.4	1.98	0.31	15.52	1.36	53
13SACZ04b	15	50.6	54	34.8	371	1.27	94.0	41	25.3	7.7	2.38	0.46	15.88	1.09	12

Note: Fission–track age is given as central ages (Galbraith & Laslett, 1993). Samples were counted dry with BX51 Olympus microscopes at 1250x magnification at the Servicio Geológico Colombiano in Bogotá and at ISTerre, Grenoble. Ages were calculated with the BINOMFIT program of Brandon (2002), using a zeta value of 274.44 ± 11.56 (2SE) and the IRMM540R uranium glass standard (15 ppm U).

*Calculated with a zeta of 303.52 ± 9.90 (2SE).

**c–axis projected track lengths.

Table 3. Santander Massif (Cepitá area) zircon fission–track data.

Sample	N	r_s (10^{+6} cm^{-2})	N_s	r_i (10^{+5} cm^{-2})	N_i	r_d (10^{+5} cm^{-2})	P(c²)	Dispersion (%)	Central Age (Ma)	±2σ	U (ppm)	±2σ
Western block												
12SACEP02	17	11.0	1640	7.19	107	3.45	0.0	73.7	264.8	110.9	233	83
12SACEP05	12	4.25	1390	6.27	205	3.40	0.0	42.7	127.5	37.8	512	73
12SACEP11	20	8.55	3329	12.3	480	3.45	1.9	19.3	142.4	21.2	142	14
12SACEP14	7	8.53	1395	10.4	170	3.46	17.4	11.7	166.7	32.7	120	19
13SACZ02	20	10.0	1917	13.5	259	3.38	2.6	22.5	145.6	25.7	159	20
13SACZ09	18	7.74	1874	12.6	305	3.40	15.9	10.3	122.8	18.3	148	17
Eastern block												
13SACZ03	10	12.7	696	101	557	3.38	6.0	14.2	24.6	3.9	1192	106
13SACZ05	20	16.8	2368	47.4	670	3.39	0.0	66.7	88.7	28.3	558	45
13SACZ07	20	3.60	1253	29.0	1010	3.39	0.0	49.9	25.1	6.3	340	23

Note: Fission–track age is given as central ages (Galbraith & Laslett, 1993). Samples were counted dry with BX51 Olympus microscopes at 1250x magnification at the Servicio Geológico Colombiano in Bogotá and at ISTerre, Grenoble. Ages were calculated with the BINOMFIT program of Brandon (2002), using a zeta value of 118.48 ± 3.85 (2SE) and the CN1 uranium glass standard (39.8 ppm U).
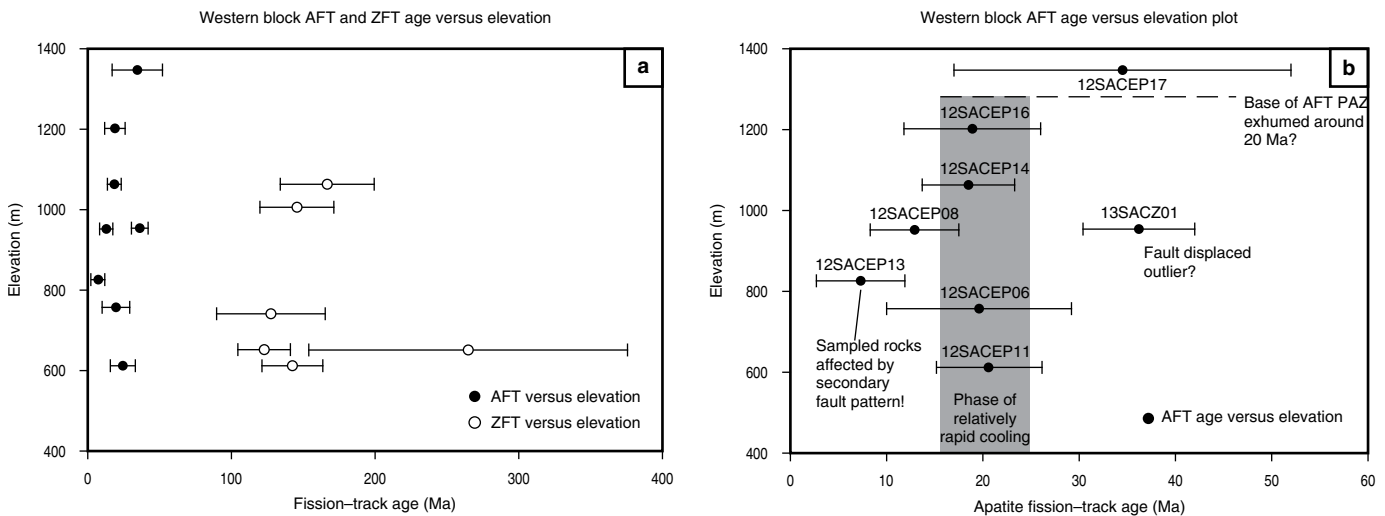

Figure 4. (a) Apatite and zircon fission–track age–elevation relationship of the western block profile in the Cepitá area of the southwestern Santander Massif. Ages are plotted with 2σ errors. **(b)** Apatite fission–track age–elevation relationship of the western block profile in the Cepitá area of the southwestern Santander Massif. Ages are plotted with 2σ errors. The base of the exhumed apatite fission–track partial annealing zones is shown with dashed line.

ZFT ages in the western block range between 123 and 265 Ma (Figure 4a; Table 3).

In the eastern profile, the AFT ages of two samples collected at the same elevation from an andesitic dike within the Bucaramanga Gneiss and the Bucaramanga Gneiss itself are 6.9 ± 2.4 Ma and 25 ± 7.7 Ma, with Dpar values of 1.98 μm and 2.38 μm and mean track lengths of 15.52 μm and 15.88 μm, respectively (Figure 2; Table 2). The ZFT ages of the three samples from the eastern block are approximately 25 Ma (samples 13SACZ03 and 07) and 89 Ma (sample 13SACZ05; Figure 2; Table 3).

Using a common pre–25 Ma thermal gradient of 30 °C/km and the age–offset of the ZFT ages of samples collected at similar elevations on both sides of the Bucaramanga Fault allows estimation of the relative uplift along the Bucaramanga Fault (Figure 5). Furthermore, the exhumed AFT and ZFT partial annealing zones can be constrained (Figures 4b, 5). The over–dispersion of single grain ages in individual samples, which is reflected by a P (χ2) value < 5% (Tables 2, 3), indicate complex grain–age distributions. Over–dispersion may be due to the intrinsic variation in the uranium concentration and radioactive decay, given that spontaneous track formation follows a Poisson
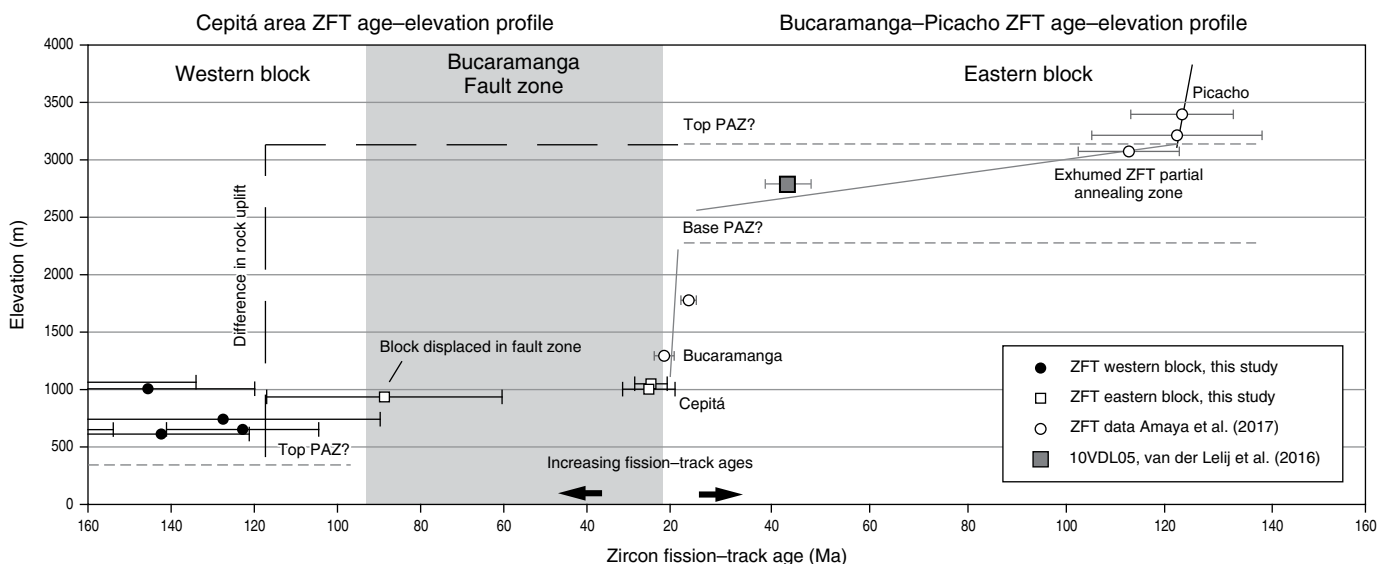
Figure 5. ZFT age–offset plot between the western and eastern blocks. This figure shows the relative uplift on both sides along the Bucaramanga Fault. Furthermore, exhumed ZFT partial annealing zones of each block can be seen.

distribution, equal to the formation of induced tracks. However, over–dispersion may also be indicative of a complex thermal history and partial annealing of fission tracks in apatite and zircon. The implication is that discordance in fission–track dating is more commonly the indication of a mixed distribution than of a poorly measured distribution. There are a number of possible reasons for this (see Galbraith & Laslett, 1993 or Galbraith, 2005 for details); however, in this study, we believe that the over–dispersion is a result of partial annealing and differences in annealing properties, as caused by variations in the chemical compositions of apatite (e.g., Donelick et al., 2005, and references therein) or variations in the radiation damage of zircon (Brandon, 1992; Garver et al., 2005).

4.2. Thermal History Modeling

We performed thermal history modeling for samples from the western profile, combining AFT age, Dpar, ZFT age, and AFT track length data. Although the track length data indicate relatively rapid cooling through the partial annealing zone (PAZ), the average Dpar values are in general >1.75 μm (Figure 6), indicating that the analyzed apatites are relatively slow annealing (Donelick et al., 2005). This condition is probably because annealing resistance increases with increasing chlorine content (Green et al., 1985). We used our track length data to constrain our QTQt models. Furthermore, the models were based on apatite fission–track age, track length, Dpar value, zircon fission–track ages, and 100 000 attempted paths. The constraint boxes for inverse modeling were placed following the forward model to match the observed fission–track ages as closely as possible and the stratigraphic constraint box between 160 Ma to 130 Ma that constrains the Jurassic
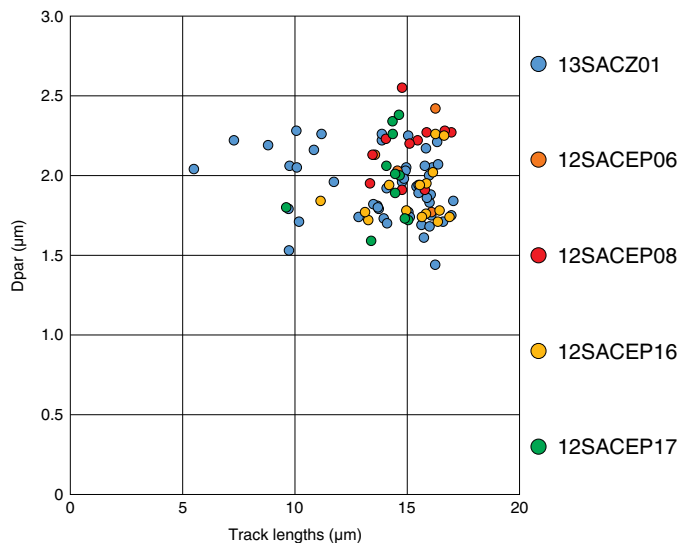

Figure 6. Plot of track length versus Dpar, showing trends defining coherent kinetic populations with values of track lengths of ca. 15 μm and Dpar > 1.5.

sedimentation (Sarmiento–Rojas et al., 2006) and between 120 Ma to 60 Ma that constrains the burial of sedimentary rocks, at least since the Late Jurassic and throughout most of the Cretaceous (Sarmiento–Rojas et al., 2006). Our track lengths data are similar to van der Lelij et al. (2016), who presented a mean AFT track length of 15.13 ± 1.03 μm for sample 10VDL22 in the study area with an AFT age of 20 Ma (Figure 2; Table 4), which we used for constraining the t–T modeling of rapidly cooled AFT grains with apparent cooling ages < ca. 25 Ma. This, in combination with AFT age, AFT Dpar, ZFT age, track length, and surface temperature data, al-

Table 4. Published fission–track data along the Bucaramanga Fault to the north of the Cepitá area.

Sample	Elevation (m)	Unit	AFT Age (Ma)	±2σ	ZFT Age (Ma)	±2σ	Reference
BC79–1	650	Pescadero Granite	13.7	1.7	93.0	10.0	Shagam et al. (1984)
BC79–6	625	Silgará Schists	18.9	2.2			Shagam et al. (1984)
10VDL22	640	Pescadero Granite	20.0	3.3	172.0	16.4	van der Lelij et al. (2016)
GC996–31	839	Silgará Schists	21.4	8.4			Caballero et al. (2013)
GC996–37	900	Silgará Schists	15.7	3.4			Caballero et al. (2013)
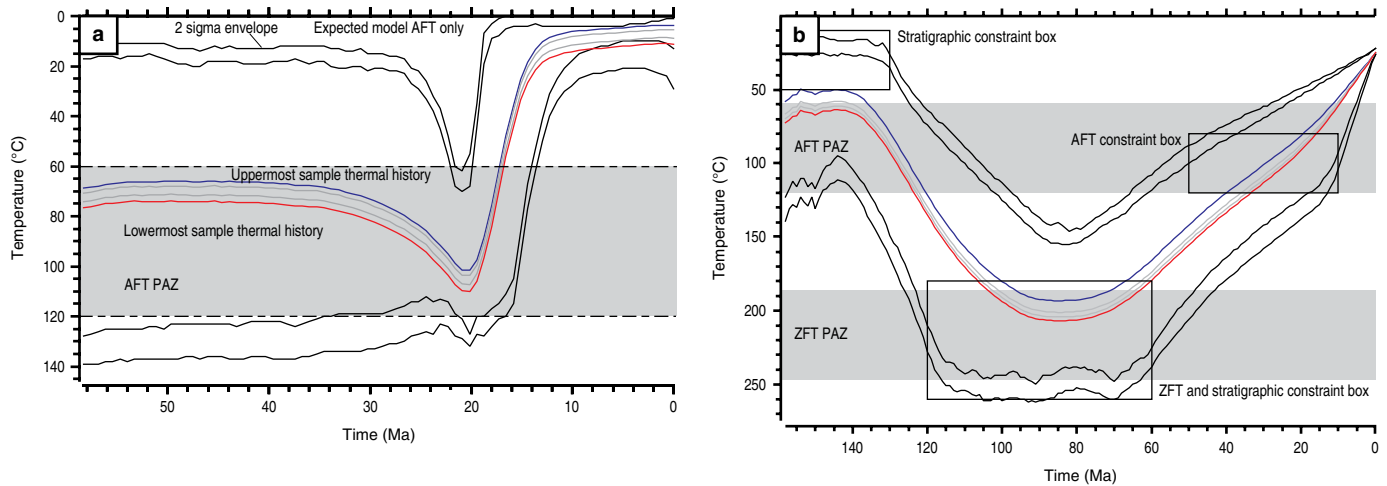
Figure 7. (a) AFT QTQt model of the western block. **(b)** ZFT QTQt model of the western block. In both plots the expected model for the thermal history solutions are shown. The profiles contain more than one sample. Any constraints are drawn as black boxes (Gallagher, 2012).

lows the presentation of a reasonable first–order expected t–T model (Figure 7). The AFT QTQt expected model shows that the western block was less affected by rapid late Oligocene – early Miocene cooling (Figure 7a) than the eastern block, despite the approximately 20 Ma cooling ages of samples 12SACEP06, 12SACEP11, 12SACEP14, and 12SACEP16. We believe this is because sample 12SACEP13, collected along the secondary fault on the western flank of the western block (Figure 2; Table 1), has a 7.3 ± 4.6 Ma cooling age. The QTQt model in Figure 7a shows an increase in cooling rates from ca. 0.5 °C/my between 50–10 Ma to ca. 5–8 °C over the past 5 to 10 my. We used the AFT data for constraining the ZFT QTQt model as shown in Figure 7b. Given that Upper Jurassic sedimentary rocks of the Girón Formation were deposited on the crystalline rocks of the western Santander Massif, we can constrain the thermal history with surface–temperature conditions between 155–140 Ma. Therefore, the western block underwent reheating between approximately 140 to 90 Ma at a rate of ca. 3 °C/my. From approximately 90 to approximately 65 Ma, the sampled rocks of the western block resided in the ZFT partial annealing zone and cooling started during the early Paleocene (Figure 7b).

4.3. Exhumation Rates

On the basis of the AFT ages, long–term exhumation rates during the Miocene – Pliocene were on the order of 0.2–0.3 km/my for the western block and 0.5–1.3 km/my for the eastern block (Figure 8). The partially reset ZFT ages of the western block indicate that the exhumation of the western block since the early Paleocene was not sufficient to exhume fully reset zircons. Because of partial annealing, no precise exhumation rates could be determined; however, these rates were on the order of 0.1–0.2 km/my. Samples 13SACZ04 and 13SACZ07 indicate that, on average, the eastern block has been exhumed at a rate of 0.3 km/my since approximately 25 Ma (Figure 8).

5. Discussion

5.1. Insights from Thermochronology

The t–T history modeling using our thermochronological data of the southwestern Santander Massif shows that the western and eastern blocks on both sides of the Bucaramanga Fault have different thermal histories. The inverse modeling of the ZFT data
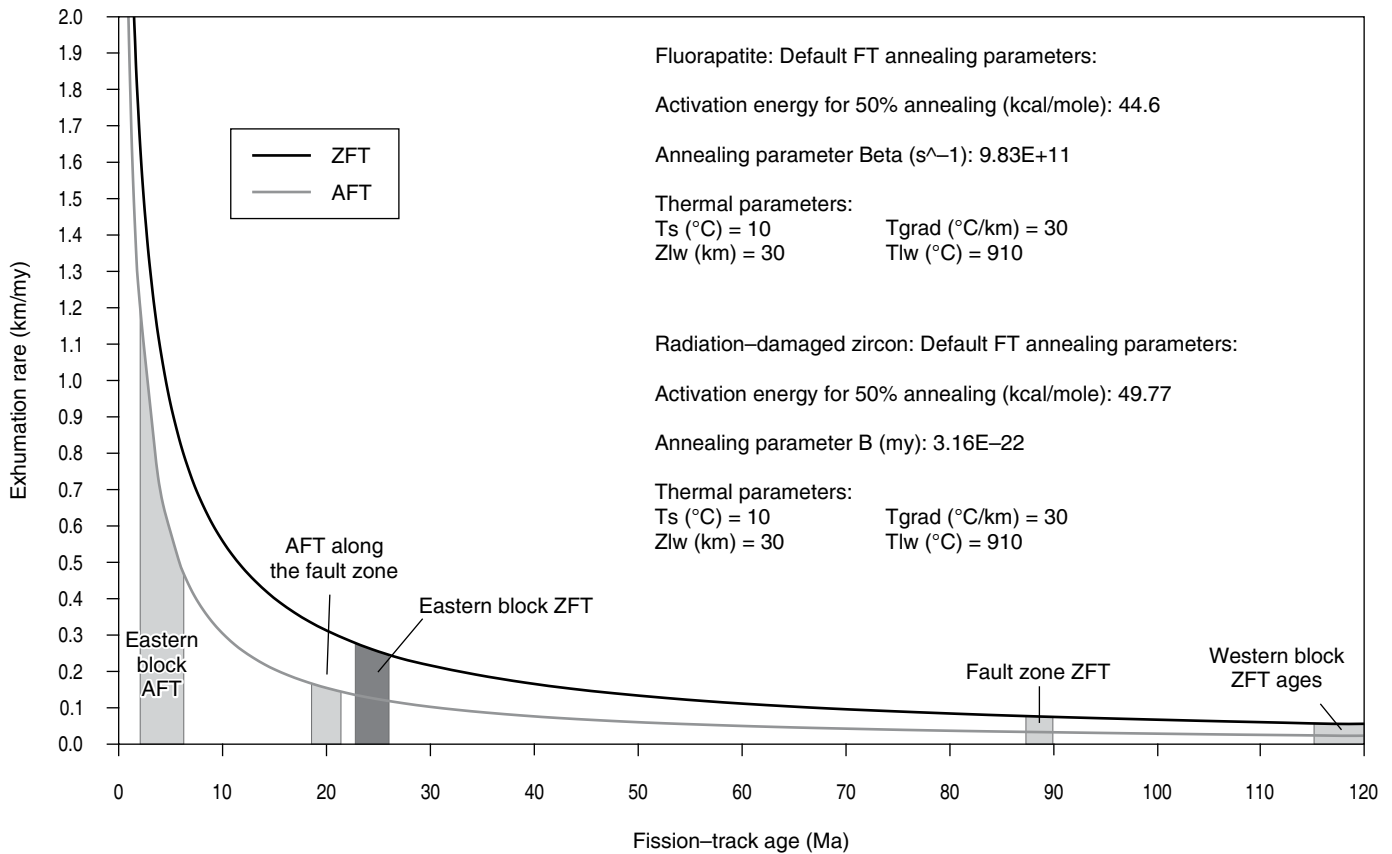
Figure 8. Relationship between fission–track age and exhumation rate determined for a 30 °C/km steady–state thermal gradient and an average surface temperature of 10 °C for the apatite and zircon fission–track system. The exhumation rates were estimated from the curves of the appropriate thermochronological system. Data obtained from the age2edot program of M. BRANDON (see Ehlers et al., 2005).

of the western block shows burial heating since the Late Jurassic, followed by nearly isothermal conditions during the Late Cretaceous and monotonic cooling that started during the early Paleocene (Figure 7b). This monotonic cooling was most likely caused by erosional exhumation of the Santander Massif and removal of overlying sedimentary cover and crystalline basement rocks.

With the exception of sample 12SACEP13, the AFT ages of the western block show a typical age–elevation trend of an exhumed AFT partial annealing zone (Figure 4b), with exhumation and cooling below approximately 120 °C occurring at ca. 20 Ma. This is consistent with the published AFT ages at low elevations (625–900 m) of Caballero et al. (2013), Shagam et al. (1984), and van der Lelij et al. (2016) along the Bucaramanga Fault zone to the north of the Cepitá area (Figure 2; Table 4). Movement on the NE–SW–oriented secondary fault pattern seems to be more recent, given the late Miocene AFT cooling age of sample 12SACEP13 at 826 m. As the western block had already cooled below ca. 120 °C during the early Miocene, this younger cooling age may be related to cooling after frictional heating in the secondary fault zone; however, more research is needed to confirm this hypothesis.

The non–annealed to partially annealed ZFT ages of the western block may indicate residence of the rocks near the top

or just above of a fossil ZFT partial annealing zone, whose base is not yet exposed in the western block. The ZFT ages of 123 Ma to 167 Ma, found in the present study at 650–1350 m in the western block are similar to ZFT ages of 120–150 Ma found at 3200–3500 m in the eastern block of the Santander Massif to the east of Bucaramanga (Amaya et al., 2017). This suggests a difference in uplift of approximately 2000 m between the western and eastern blocks. Based on the late Oligocene 25 Ma ZFT ages of samples 13SACZ03 and 13SACZ07 at similar elevations (1003 and 1050 m) of the eastern block in the Cepitá area (Table 3) and the approximately 25–20 Ma ZFT ages in the lower part of the Bucaramanga–Picacho profile of Amaya et al. (2017), the differential uplift started during the late Oligocene to early Miocene (Figure 5) but may have continued until the late Miocene – Pliocene, given the young AFT cooling ages of Amaya et al. (2017) to the east of the Bucaramanga fault.

The difference in the AFT ages of samples 13SACZ04a and 13SACZ04b and the ZFT age of sample 13SACZ03 from the eastern block at similar elevations of 1050 and 1022 m, respectively, is interesting sample 13SACZ04b was collected from the Bucaramanga Gneiss (Table 1) and shows an age of 25.3 ± 7.7 Ma during the rapid late Oligocene – early Miocene cooling also observed in the ZFT data. However, sample 13SACZ04a

was collected from an andesitic dike and has an apparent AFT cooling age of 6.9 ± 2.4 Ma (Tables 1, 2). Even if this age is not very well constrained, it suggests possibly short–lived magmatic activity, and hydrothermal fluid flow, in this part of the Santander Massif. The relation of this late Miocene magmatic activity to the formation of late Miocene hydrothermal gold mineralization in the California Vetas area of the Santander Massif (e.g., Mantilla–Figueroa et al., 2013; Urueña, 2014) or the volcanic activity at the same time in the Eastern Cordillera Paipa–Iza Complex (Bernet et al., 2016) is not clear at this stage and warrants further research. Nonetheless, we believe that based on field evidence this very minor magmatic activity in the study area did not affect the apatites of sample 13SACZ4b, and that the AFT age of that sample records exhumation cooling.

5.2. Regional Tectonic Control on Cooling and Exhumation

The thermal history model (Figure 7b), in combination with the AFT and ZFT age–elevation data of the western and eastern blocks discussed above, reveal a four–stage thermal history in connection with regional tectonic events for the southwestern Santander Massif. After the 60 my phase of subsidence and burial heating (stage 1) between the Late Jurassic and Late Cretaceous, cooling of the crystalline rocks of the Santander Massif started during the Late Cretaceous – early Paleocene. We believe this initiation of cooling was related to the Late Cretaceous accretion of an island–arc to the west of South America (e.g., Jaillard et al., 2000) and interaction of the Caribbean Plate with the western margin of South America (Bayona et al., 2013), which led to surface uplift and erosion in the area of the Santander Massif, as documented in the surrounding sedimentary basins, such as the Cesar Basin sedimentary record (e.g., lithic fragments in the Late Cretaceous to Paleocene Colón Formation) to the north of the Santander Massif (Figure 1; Ayala–Calvo et al., 2009, Bayona et al., 2013; Villamil, 1999) or the Nuevo Mundo Syncline to the west of the Santander Massif (Figure 1; Caballero et al., 2013).

The third stage of the thermal history is marked by rapid cooling and exhumation along the Bucaramanga Fault in the Santander Massif during the collision of the Panamá–Chocó Block with the northwestern South American plate at approximately 25 Ma (Farris et al., 2011; O'Dea et al., 2016), possibly as a result of the Farallón Plate break–up also at approximately 25 Ma (Taboada et al. 2000). This means the rocks were already being exhumed during the Oligocene, but exhumation particularly accelerated in the eastern block during the late Oligocene. This result is consistent with previously published thermochronological data reported by Amaya et al. (2017) from samples collected to the west of the Suratá Fault and near Bucaramanga, which indicate that cooling caused by exhumation of the PAZ occurred between 25 and 20 Ma, and from plutonic rocks that

intruded the Bucaramanga Gneiss and Silgará Schists, which also indicate that the exhumation of the Santander Massif was already underway during the Oligocene (Caballero et al., 2013). Furthermore, late Oligocene to early Miocene exhumation is a common phenomenon in the northern Andes and has already been described for the Antioquian Batholith of the Central Cordillera (Restrepo–Moreno et al., 2009), the Caparo Block of the southwestern Mérida Andes (Bermúdez et al., 2010; Kohn et al., 1984), and the Sierra Nevada de Santa Marta of the northern Santander Massif (Figure 9b).

Finally, late Miocene cooling ages, as observed along the secondary NE–SW–oriented fault pattern (sample 12SACEP13), and minor magmatic activity (sample 13SAC-Z04A) in the Santander Massif are approximately contemporaneous with the initiation of significant surface uplift of the Eastern Cordillera (Mora et al., 2009). Such young AFT cooling ages have also been found along the Boconó Fault in the Mérida Andes (Bermúdez et al., 2010, 2011; Kohn et al., 1984). Therefore, a regional tectonic driver was also likely responsible for this latest exhumation stage in the Santander Massif, which may have been related to the subduction of the Caribbean Plate and slab break–off (Vargas & Mann, 2013). However, we have not ruled out that the late Miocene cooling ages in the western Santander Massif indicate the initiation of exhumation in the eastern Santander Massif during the Pliocene – Pleistocene related to the buttress effect of the collision of the Chocó Block as described by Velandia (2017).

5.3. Topographic Evolution

The Bucaramanga Fault played a very important role in the exhumation of the crystalline basement and surface uplift of the Santander Massif to greater than 3600–4530 m in elevation, generating asymmetric topography as seen in the eastern and western blocks of the Bucaramanga Fault and other fault blocks within the Santander Massif (Amaya et al., 2017). The topography observed today in the Santander Massif is the result of all of the accumulated deformation of the massif since the beginning of its uplift by inversion of geological structures in the Late Cretaceous – early Paleocene until the Pliocene – Pleistocene when faulted structures in a NE direction accommodated the deformation, with displacement in course, possibly due to the collision and buttress effect of the Chocó Block (Velandia, 2017; Villamizar, 2017). Recently published studies have identified that the structure of the Santander Massif is composed of tectonic blocks (e.g., Amaya et al., 2017; van der Lelij et al., 2016), and in this study, we identified two tectonic blocks, namely, the western and eastern blocks of the Bucaramanga Fault, each with different thermal histories, as described above. Using our thermochronological data, a new model for the topographic evolution of the Santander Massif in the Cepitá area is proposed (Figures 9, 10). We believe that
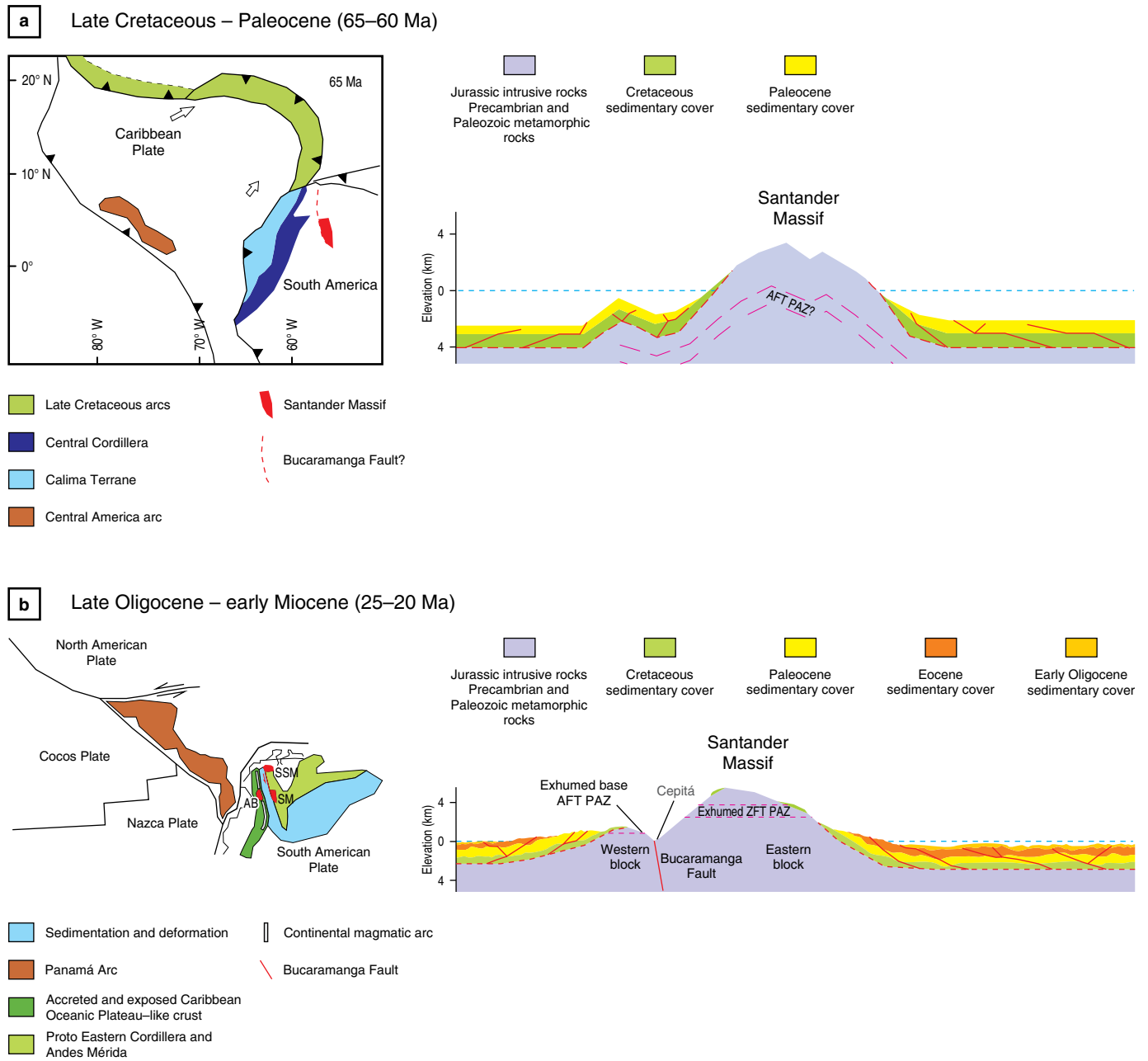
Figure 9. Model geodynamic topographic evolution of the Santander Massif. Crustal ––scale cross–– section from 65 Ma to 20 Ma, showing the relationship between exhumation and topographic evolution of Santander Massif and regional tectonics. **(a)** In Late Cretaceous and early Paleocene times, the collision of the Caribbean Plate with the northwestern South American continental margin produced reactivation of intraplate structures that contributed to the exhumation and surface uplift of the Santander Massif. **(b)** Regional tectonics setting, showing the collision of the Panamá Arc with the northwestern South American continental margin and its effects on the exhumation and topographic evolution of the Santander Massif. (SM) Santander Massif; (SNSM) Sierra Nevada de Santa Marta; (AB) Antoquian Batholith. (a) Position of the Caribbean Plate, Central America Arc, and direction of movement of the plates is taken and modified by Spikings et al. (2015). (b) Position of the Caribbean Plate, the Panamá Arc, and directions of movement of the plates, is taken an modified by Boschman et al. (2014).

the topographic development of the Santander Massif initiated during the Late Cretaceous – early Paleocene, although this development occurred along inversion structures and was not strong (Figure 9a). In contrast to the Mérida Andes, which reached their present–day elevation by the late Miocene (Ber-

múdez et al., 2017), the present–day topographic elevations of the Santander Massif were probably in place during the late Oligocene – early Miocene (Figure 9b), when the Panamá arc collided with northwestern South America. The surface uplift of the eastern block reached overall much higher surface

Figure 10. Photograph of the eastern block Bucaramanga Fault in the Cepitá area showing position of the paleozone of the partial annealing zone of the zircon fission track (PAZ–ZFT).

elevations than that of the western block (Figure 10), likely influenced by the isostatic response of the crystalline rocks of the eastern block, which was three times faster than that of the crystalline rocks of the western block, which are covered with sedimentary rocks (Braun et al., 2014).

6. Conclusion

Our main conclusions about the tectonic and thermal evolution of the Santander Massif from this thermochronological study are summarized as follows. (i) Cooling of the Santander Massif crystalline rocks, related to erosional exhumation, began during the Late Cretaceous – early Paleocene at approximately 65–60 Ma. (ii) A second cooling phase related to Bucaramanga Fault activity and erosion caused by the Panamá–Chocó Block collision with northwestern South America started during the late Oligocene to early Miocene. (iii) The latest phase of cooling occurred during the Pliocene – Pleistocene but can primarily be observed along the secondary fault pattern in the Santander Massif. All three phases of faster or slower cooling can be related to regional tectonic events in the northern Andes.

Our dataset furthermore illustrates that exhumation of the Santander Massif basement rocks on both sides of the Bucaramanga Fault was asymmetric because there is an approximately 2000 m difference in elevation between rocks with similar ZFT cooling ages in the eastern and western blocks, and the overall surface elevations of the eastern block are much higher than those of the western block.

Acknowledgments

References

Amaya, S., Zuluaga, C. & Bernet, M. 2017. New fission–track age constraints on the exhumation of the central Santander Massif: Implications for the tectonic evolution of the northern Andes, Colombia. Lithos, 282–283: 388–402. https://doi.org/10.1016/j.lithos.2017.03.019

Ayala–Calvo, R.C., Bayona, G., Ojeda–Marulanda, C., Cardona, A., Valencia, V., Padrón, C.E., Yoris, F., Mesa–Salamanca, J. & García, A. 2009. Estratigrafía y procedencia de las unidades comprendidas entre el Campaniano y el Paleógeno en la Subcuenca de Cesar: Aportes a la evolución tectónica del área. Geología Colombiana, (34): 3–33.

Bayona, G., Cardona, A., Jaramillo, C., Mora, A., Montes, C., Caballero, V., Mahecha, H., Lamus, F., Montenegro, O., Jiménez, G., Mesa, A. & Valencia, V. 2013. Onset of fault reactivation in the Eastern Cordillera of Colombia and proximal Llanos Basin; Response to Caribbean–South American convergence in early Palaeogene time. In: Nemčok, M., Mora, A. & Cosgrove, J.W. (editors), Thick–skin–dominated orogens: From initial inversion to full accretion. Geological Society of London, Special Publication 377, p. 285–314. https://doi.org/10.1144/SP377.5

Bermúdez, M.A., Kohn, B.P., van der Beek, P.A., Bernet, M., O'Sullivan, P.B. & Shagam, R. 2010. Spatial and temporal patterns of exhumation across the Venezuelan Andes: Implications for Cenozoic Caribbean geodynamics. Tectonics, 29(5): 1–21. https://doi.org/10.1029/2009TC002635

Bermúdez, M.A., van der Beek, P. & Bernet, M. 2011. Asynchronous Miocene – Pliocene exhumation of the central Venezuelan Andes. Geology, 39(2): 139–142. https://doi.org/10.1130/G31582.1

Bermúdez, M.A., van der Beek, P. & Bernet, M. 2013. Strong tectonic and weak climatic control on exhumation rates in the Venezuelan Andes. Lithosphere, 5(1): 3–16. https://doi.org/10.1130/L212.1

Bermúdez, M.A., Hoorn, C., Bernet, M., Carrillo, E., van der Beek, P.A., Garver, J.I., Mora, J.L. & Mehrkian, K. 2017. The detrital record of late–Miocene to Pliocene surface uplift and exhumation of the Venezuelan Andes in the Maracaibo and Barinas Foreland Basins. Basin Research, 29(S1): 370–395. https://doi.org/10.1111/bre.12154

Bernet, M. 2009. A field–based estimate of the zircon fission–track closure temperature. Chemical Geology, 259(3–4): 181–189. https://doi.org/10.1016/j.chemgeo.2008.10.043

Bernet, M., Urueña, C., Amaya, S. & Peña, M.L. 2016. New thermo and geochronological constraints on the Pliocene – Pleistocene eruption history of the Paipa–Iza Volcanic Complex, Eastern Cordillera, Colombia. Journal of Volcanology and Geothermal Research, 327(15): 299–309. https://doi.org/10.1016/j.jvolgeores.2016.08.013

Boschman, L.M., van Hinsbergen, D.J.J., Torsvik, T.H., Spakman, W. & Pindell, J.L. 2014. Kinematic reconstruction of the Caribbean region since the Early Jurassic. Earth–Science Reviews, 138: 102–136. https://doi.org/10.1016/j.earscirev.2014.08.007

Brandon, M.T. 1992. Decomposition of fission–track grain–age distributions. American Journal of Science, 292(8): 535–564. https://doi.org/10.2475/ajs.292.8.535

Brandon, M.T. 2002. Decomposition of mixed grain age distributions using BINOMFIT. On Track, 24: 13–19.

Brandon, M.T., Roden–Tice, M.K. & Garver, J.I. 1998. Late Cenozoic exhumation of the Cascadia accretionary wedge in the Olympic Mountains, Northwest Washington State. Geological Society of America Bulletin, 110(8): 985–1009. https://doi.org/10.1130/0016-7606(1998)110<0985:LCEOTC>2.3.CO;2

Braun, J., Simon–Labric, T., Murray, K.E. & Reiners, P.W. 2014. Topographic relief driven by variations in surface rock density. Nature Geoscience, 7: 534–540. https://doi.org/10.1038/ngeo2171

Burtner, R.L., Nigrini, A. & Donelick, R.A. 1994. Thermochronology of Lower Cretaceous source rocks in the Idaho–Wyoming Thrust Belt. American Association of Petroleum Geologists Bulletin, 78(10): 1613–1636.

Caballero, V., Mora, A., Quintero, I., Blanco, V., Parra, M., Rojas, L.E., López, C., Sánchez, N., Horton, B.K., Stockli, D.F. & Duddy, I. 2013. Tectonic controls on sedimentation in an intermontane hinterland basin adjacent to inversion structures: The Nuevo Mundo Syncline, Middle Magdalena Valley, Colombia. In: Nemčok, M., Mora, A. & Cosgrove, J.W. (editors), Thick–skin–dominated orogens: From initial inversion to full accretion. Geological Society of London, Special Publication 377, p. 315–342. London. https://doi.org/10.1144/SP377.12

Colletta, B., Roure, F., de Toni, B., Loureiro, D., Passalacqua, H. & Gou, Y. 1997. Tectonic inheritance, crustal architecture, and contrasting structural styles in the Venezuela Andes. Tectonics, 16(5): 777–794. https://doi.org/10.1029/97TC01659

Colmenares, L. & Zoback, M.D. 2003. Stress field and seismotectonics of northern South America. Geology, 31(8): 721–724. https://doi.org/10.1130/G19409.1

Donelick, R.A., O'Sullivan, P.B. & Ketcham, R.A. 2005. Apatite fission–track analysis. Reviews in Mineralogy and Geochemistry, 58(1): 49–94. https://doi.org/10.2138/rmg.2005.58.3

Ehlers, T.A., Chaudhri, T., Kumar, S., Fuller, C.W., Willett, S.D., Ketcham, R.A., Brandon, M.T., Belton, D.X., Kohn, B.P., Gleadow, A.J.W., Dunai, T.J. & Fu, F.Q. 2005. Computational tools for low–temperature thermochronometer interpretation. Reviews in Mineralogy and Geochemistry, 58(1): 589–622. https://doi.org/10.2138/rmg.2005.58.22

Farris, D.W., Jaramillo, C., Bayona, G., Restrepo–Moreno, S.A., Montes, C., Cardona, A., Mora, A., Speakman, R.J., Glascock, M.D. & Valencia, V. 2011. Fracturing of the Panamanian Isthmus during initial collision with South America. Geology, 39(11): 1007–1010. https://doi.org/10.1130/G32237.1

Galbraith, R.F. 2005. Statistics for fission tracks analysis. Chapman & Hall/CRC, 240 p. Boca Ratón, Costa Rica.

Galbraith, R.F. & Laslett, G.M. 1993. Statistical models for mixed fission track ages. Nuclear tracks and radiation measurements, 21(4): 459–470. https://doi.org/10.1016/1359-0189(93)90185-C

Gallagher, K., 2012. Transdimensional inverse thermal history modeling for quantitative thermochronology. Journal of Geophysical Research: Solid Earth, 117(B2): 1–16. https://doi.org/10.1029/2011JB008825

Garver, J.I., Reiners, P.W., Walker, L.J., Ramage, J.M. & Perry, S.E. 2005. Implications for timing of Andean uplift from thermal resetting of radiation–damaged zircon in the Cordillera Huayhuash, northern Peru. The Journal of Geology, 113(2): 117–138.

Goldsmith, R., Marvin, R.F. & Mehnert, H.H. 1971. Radiometric ages in the Santander Massif, Eastern Cordillera, Colombian Andes. U. S. Geological Survey, Professional Paper, 750–D: D44–D49.

Green, P.F., Duddy, I.R., Gleadow, A.J.W., Tingate, P.R. & Laslett, G.M. 1985. Fission– track annealing in apatite: Track length measurements and the form of the Arrhenius plot. Nuclear Tracks and Radiation Measurements, 10(3): 323–328. https://doi.org/10.1016/0735-245X(85)90121-8

Different Levels of Exhumation across the Bucaramanga Fault in the Cepitá Area of the Southwestern Santander Massif, Colombia

Quaternary

Neogene

Paleogene

Cretaceous

Jurassic

Hoorn, C., Wesselingh, F.P., ter Steege, H., Bermúdez, M.A., Mora, A., Sevink, J., Sanmartín, I., Sánchez–Meseguer, A., Anderson, C.L., Figueiredo, J.P., Jaramillo, C., Riff, D., Negri, F.R., Hooghiemstra, H., Lundberg, J., Stadler, T., Särkinen, T. & Antonelli, A. 2010. Amazonia through time: Andean uplift, climate change, landscape evolution, and biodiversity. Science, 330(6006): 927–931. https://doi.org/10.1126/science.1194585

Jaillard, E., Hérail, G., Monfret, T., Díaz–Martínez, E., Baby, P., Lavenu, A. & Dumont, J.F. 2000. Tectonic evolution of the Andes of Ecuador, Peru, Bolivia and northernmost Chile. In: Cordani, U.G., Milani, E.J., Thomaz–Filho, A. & Campos, D.A. (editors), Tectonic evolution of South America, p. 481–559. Rio de Janeiro.

Kohn, B.P., Shagam, R., Banks, P.O. & Burkley, L.A. 1984. Mesozoic–Pleistocene fission–track ages on rocks of the Venezuelan Andes and their tectonic implications. In: Bonini, W.E., Hargraves, R.B. & Shagam, R. (editors), The Caribbean–South American Plate boundary and regional tectonics, Geological Society of America, Memoir 162, p. 365–384. https://doi.org/10.1130/MEM162-p365

Mann, P., Escalona, A. & Castillo, M.V. 2006. Regional geologic and tectonic setting of the Maracaibo supergiant Basin, western Venezuela. American Association of Petroleum Geologists Bulletin, 90(4): 445–477. https://doi.org/10.1306/10110505031

Mantilla–Figueroa, L.C., Bissig, T., Valencia, V. & Hart, C.J.R. 2013. The magmatic history of the Vetas–California mining district, Santander Massif, Eastern Cordillera, Colombia. Journal of South American Earth Sciences, 45: 235–249. https://doi.org/10.1016/j.jsames.2013.03.006

Mapes, B.E., Warner, T.T., Xu, M. & Negri, A.J. 2003. Diurnal patterns of rainfall in northwestern South America. Part I: Observations and context. Monthly Weather Review, 131(5): 799–812. https://doi.org/10.1175/1520-0493(2003)131<0799:DPORIN>2.0.CO;2

Mora, A., Gaona, T., Kley, J., Montoya, D., Parra, M., Quiroz, L.I., Reyes, G. & Strecker, M.R. 2009. The role of inherited extensional fault segmentation and linkage in contractional orogenesis: A reconstruction of Lower Cretaceous inverted rift basins in the Eastern Cordillera of Colombia. Basin Research, 21(1): 111–137. https://doi.org/10.1111/j.1365-2117.2008.00367.x

Mora, A., Casallas, W., Ketcham, R.A., Gómez, D., Parra, M., Namson, J., Stockli, D.F., Almendral, A., Robles, W. & Ghorbal, B. 2015. Kinematic restoration of contractional basement structures using thermokinematic models: A key tool for petroleum system modeling. American Association of Petroleum Geologists Bulletin, 99(8): 1575–1598. https://doi.org/10.1306/04281411108

O'Dea, A., Lessios, H.A., Coates, A.G., Eytan, R.I., Restrepo–Moreno, S., Cione, A.L., Collins, L.S., de Queiroz, A., Farris, D.W., Norris, R.D., Stallard, R.F., Woodburne, M.O., Aguilera, O., Aubry, M.P., Berggren, W.A., Budd, A.F., Cozzuol, M.A., Coppard, S.E., Duque–Caro, H., Finnegan, S., Gasparini, G.M., Grossman, E.L., Johnson, K.G., Keigwin, L.D., Knowlton, N., Leigh, E.G., Leonard–Pingel, J.S., Marko, P.B., Pyenson, N.D., Rachello–Dolmen, P.G., Soibelzon, E., Soibelzon, L., Todd, J.A., Vermeij, G.J. & Jackson, J.B.C. 2016. Formation of Isthmus of Panama. Science Advances, 2(8): 1–11. https://doi.org/10.1126/sciadv.1600883

Parra, M., Mora, A., López, C., Rojas, L.E. & Horton, B.K. 2012. Detecting earliest shortening and deformation advance in thrust belt hinterlands: Example from the Colombian Andes. Geology, 40(2): 175–178. https://doi.org/10.1130/G32519.1

Restrepo–Moreno, S.A., Foster, D.A., Stockli, D.F. & Parra–Sánchez, L.N. 2009. Long–term erosion and exhumation of the "Altiplano Antioqueño", northern Andes (Colombia) from apatite (U–Th)/He thermochronology. Earth and Planetary Science Letters, 278(1–2): 1–12. https://doi.org/10.1016/j.epsl.2008.09.037

Sánchez, J., Horton, B.K., Tesón, E., Mora, A., Ketcham, R.A. & Stockli, D.F. 2012. Kinematic evolution of Andean fold–thrust structures along the boundary between the Eastern Cordillera and Middle Magdalena Valley Basin, Colombia. Tectonics, 31(3): 24 p. https://doi.org/10.1029/2011TC003089

Sarmiento–Rojas, L.F., van Wess, J.D. & Cloetingh, S. 2006. Mesozoic transtensional basin history of the Eastern Cordillera, Colombian Andes: Inferences from tectonic models. Journal of South American Earth Sciences, 21(4): 383–411. https://doi.org/10.1016/j.jsames.2006.07.003

Shagam, R., Khon, B.P., Banks, P.O., Dasch, L.E., Vargas, R., Rodríguez, G.I. & Pimentel, N. 1984. Tectonic implications of Cretaceous – Pliocene fission–track ages from rocks of the circum–Maracaibo Basin region of western Venezuela and eastern Colombia. In: Bonini, W.E., Hargraves, R.B. & Shagam, R. (editors), The Caribbean–South American Plate boundary and regional tectonics. Geological Society of America, Memoir 162, p. 385–412. https://doi.org/10.1130/MEM162-p385

Spikings, R., Cochrane, R., Villagómez, D., van der Lelij, R., Vallejo, C., Winkler, W. & Beate, B. 2015. The geological history of northwestern South America: From Pangaea to the early collision of the Caribbean Large Igneous Province (290–75 Ma). Gondwana Research, 27(1): 95–139. https://doi.org/10.1016/j.gr.2014.06.004

Taboada, A., Rivera, L.A., Fuenzalida, A., Cisternas, A., Philip, H., Bijwaard, H., Olaya, J. & Rivera, C. 2000. Geodynamics of the northern Andes: Subductions and intracontinental deformation (Colombia). Tectonics, 19(5): 787–813. https://doi.org/10.1029/2000TC900004

Urueña, C.L. 2014. Metamorfismo, exhumación y termocronología del Neis de Bucaramanga. (Macizo de Santander, Colombia). Master thesis, Universidad Nacional de Colombia, 191 p. Bogotá.

van der Lelij, R., Spikings, R.A. & Mora, A. 2016. Thermochronology and tectonics of the Mérida Andes and the Santander Massif, NW South America. Lithos, 248–251: 220–239. https://doi.org/10.1016/j.lithos.2016.01.006

Vargas, C.A. & Mann, P. 2013. Tearing and breaking off of subducted slabs as the result of collision of the Panama Arc–indenter with northwestern South America. Bulletin of the Seismological Society of America, 103(3): 2025–2046. https://doi.org/10.1785/0120120328

Velandia, F. 2017. Cinemática de las fallas mayores del Macizo de Santander–énfasis en el modelo estructural y temporalidad al sur de la Falla de Bucaramanga, Colombia. Doctoral thesis, Universidad Nacional de Colombia, 222 p. Bogotá.

Villagómez, D., Spikings, R., Mora, A., Guzmán, G., Ojeda, G., Cortés, E. & van der Lelij, R. 2011. Vertical tectonics at a continental crust–oceanic plateau plate boundary zone: Fission track thermochronology of the Sierra Nevada de Santa Marta, Colombia. Tectonics, 30(4): 1–18. https://doi.org/10.1029/2010TC002835

Villamil, T. 1999. Campanian – Miocene tectonostratigraphy, depocenter evolution and basin development of Colombia and western Venezuela. Palaeogeography, Palaeoclimatology, Palaeoecology, 153(1–4): 239–275. https://doi.org/10.1016/S0031-0182(99)00075-9

Villamizar, N. 2017. Historia de exhumación del bloque este de la Falla de Bucaramanga usando termocronología de baja temperatura, Santander, Colombia. Master thesis, Universidad Nacional de Colombia, 112 p. Bogotá.

Willett, S.D. & Brandon, M.T. 2013. Some analytical methods for converting thermochronometric age to erosion rate. Geochemistry, Geophysics, Geosystems, 14(1): 209–222. https://doi.org/10.1029/2012GC004279

Zuluaga, C.A. & López, J.A. 2018. Ordovician orogeny and Jurassic low–lying orogen in the Santander Massif, northern Andes (Colombia). In: Cediel, F. & Shaw, R.P. (editors), Geology and tectonics of northwestern South America: The Pacific–Caribbean–Andean junction. Series: Frontiers in Earth Sciences. p. 195–250. Springer. https://doi.org/10.1007/978-3-319-76132-9_4
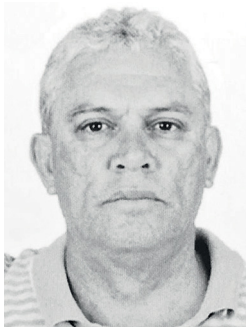
Explanation of Acronyms, Abbreviations, and Symbols:

AFT   Apatite fission track
PAZ   Partial annealing zone

ZFT   Zircon fission track

Authors' Biographical Notes

Sergio AMAYA–FERREIRA is a geologist at the Universidad Nacional de Colombia, Bogotá, and is also a specialist in environmental engineering at the Universidad Industrial de Santander. He received his Master of Science degree in geology from the Universidad Nacional de Colombia Sede Bogotá, and a Doctoral degree in geosciences from the same university. Dr. AMAYA's main research interest is the evolution of mountain ranges and sedimentary basins using low–temperature thermochronology (AFT and ZFT) and provenance analysis. He has worked as an associate professor at the School of Geology at the Universidad Industrial de Santander and as a specialized geologist in the fission–track laboratory at the Servicio Geológico Colombiano. He has also guided the following research projects in thermochronology and geochronology: "Structure and geological evolution of the crystalline basement of the Santander Massif, Eastern Cordillera, Colombia", "Petrological characterization of the Berlin Orthogneiss Unit, Santander Massif, Colombia", and "Evaluation of thermal maturity of gas associated with coals of the Umir Formation in the Middle Magdalena Valley and of the Guaduas Formation in the Umbita Syncline, Eastern Cordillera, Colombia". The first two projects have contributed to broadening our understanding of the evolution of the northern Andes in the South American northwestern fringe, which remains under discussion. The thermal maturity assessment projects have contributed to determining the potential of unconventional coal bed methane hydrocarbons in Colombia's coal basins. Currently, Dr. AMAYA is a member of the Grupo de Exploración de Minerales Metálicos in the Dirección de Recursos Minerales of the Servicio Geológico Colombiano and is currently working on a research project concerning the "application of multidisciplinary approaches, petrological, geochronological, and thermochronological, to the exploration of deposits".

Carlos Augusto ZULUAGA is an assistant professor and researcher in the Departamento de Geociencias of the Universidad Nacional de Colombia. He works on petrology applied to crustal evolution, thermodynamic modeling, and the tectonic evolution of the northern Andes.

Matthias BERNET has a PhD in geology from Yale University, USA. Since 2010, he has been the advisor of the thermochronology laboratory at the Servicio Geológico Colombiano, collaborated on several research projects of the Servicio Geológico Colombiano and helped with the implementation of the research facilities of the "Investigaciones y Aplicaciones Nucleares y Geocronológicas" Group. He is an expert in using detrital thermochronology, clastic sedimentology, and multi–disciplinary provenance analyses to study the exhumation histories of mountain belts in the northern Andes of Colombia and Venezuela, the European Alps, the Himalaya, and the Tibetan Plateau. Currently, he is the director of the ISTerre Thermochronology Laboratory at the Université Grenoble Alpes in France.

Quaternary

Neogene

Paleogene

Cretaceous

Jurassic